Global Ecology and Biogeography, (Global Ecol. Biogeogr.) (2014) **23**, 297–310

A Journal of Macroecology

Global Ecology and Biogeography

RESEARCH PAPER

Carbon stock and density of northern boreal and temperate forests

Martin Thurner[1]*, Christian Beer[1,2], Maurizio Santoro[3], Nuno Carvalhais[1,4], Thomas Wutzler[1], Dmitry Schepaschenko[5], Anatoly Shvidenko[5], Elisabeth Kompter[1], Bernhard Ahrens[1], Shaun R. Levick[1] and Christiane Schmullius[6]

[1]*Max Planck Institute for Biogeochemistry (MPI-BGC), Hans-Knöll-Straße 10, D-07745 Jena, Germany,* [2]*Department of Applied Environmental Science (ITM) and the Bolin Centre for Climate Research, Stockholm University, SE-106 91 Stockholm, Sweden,* [3]*Gamma Remote Sensing, Worbstraße 225, CH-3073 Gümligen, Switzerland,* [4]*Universidade Nova de Lisboa, Faculdade de Ciências e Tecnologia (FCT), 2829-516 Caparica, Portugal,* [5]*International Institute for Applied Systems Analysis (IIASA), Schlossplatz 1, A-2361 Laxenburg, Austria,* [6]*Friedrich-Schiller-University (FSU), Institute of Geography, Earth Observation, Grietgasse 6, D-07743 Jena, Germany*

*Correspondence: Martin Thurner, Max Planck Institute for Biogeochemistry (MPI-BGC), Hans-Knöll-Straße 10, D-07745 Jena, Germany. E-mail: mthurn@bgc-jena.mpg.de

ABSTRACT

Aim To infer a forest carbon density map at 0.01° resolution from a radar remote sensing product for the estimation of carbon stocks in Northern Hemisphere boreal and temperate forests.

Location The study area extends from 30° N to 80° N, covering three forest biomes – temperate broadleaf and mixed forests (TBMF), temperate conifer forests (TCF) and boreal forests (BFT) – over three continents (North America, Europe and Asia).

Methods This study is based on a recently available growing stock volume (GSV) product retrieved from synthetic aperture radar data. Forest biomass and spatially explicit uncertainty estimates were derived from the GSV using existing databases of wood density and allometric relationships between biomass compartments (stem, branches, roots, foliage). We tested the resultant map against inventory-based biomass data from Russia, Europe and the USA prior to making intercontinent and interbiome carbon stock comparisons.

Results Our derived carbon density map agrees well with inventory data at regional scales ($r^2 = 0.70$–0.90). While 40.7 ± 15.7 petagram of carbon (Pg C) are stored in BFT, TBMF and TCF contain 24.5 ± 9.4 Pg C and 14.5 ± 4.8 Pg C, respectively. In terms of carbon density, we found 6.21 ± 2.07 kg C m^{-2} retained in TCF and 5.80 ± 2.21 kg C m^{-2} in TBMF, whereas BFT have a mean carbon density of 4.00 ± 1.54 kg C m^{-2}. Indications of a higher carbon density in Europe compared with the other continents across each of the three biomes could not be proved to be significant.

Main conclusions The presented carbon density and corresponding uncertainty map give an insight into the spatial patterns of biomass and stand as a new benchmark to improve carbon cycle models and carbon monitoring systems. In total, we found 79.8 ± 29.9 Pg C stored in northern boreal and temperate forests, with Asian BFT accounting for 22.1 ± 8.3 Pg C.

Keywords

Boreal forest, carbon density map, carbon monitoring, forest biomass, forest carbon stocks, global carbon cycle, growing stock volume, SAR remote sensing, temperate forest.

INTRODUCTION

Terrestrial vegetation plays an important role within the global carbon cycle and hence the earth system, as it sequesters atmospheric carbon dioxide and is thus able to mitigate global warming (Denman *et al.*, 2007; Bonan, 2008). Biomass dynamics reflect the potential of vegetation to act as a carbon sink over the long term, as they integrate photosynthesis, autotrophic respiration and litterfall fluxes. However, the interannual variability of carbon fluxes remains relatively unexplored (Wolf *et al.*,

DOI: 10.1111/geb.12125
http://wileyonlinelibrary.com/journal/geb

2011), mainly due to the absence of consistent spatial information on biomass (Bellassen *et al.*, 2011). Lack of knowledge about the initial condition of vegetation biomass is one important reason for the large discrepancies in the projected land carbon sink between coupled climate–carbon cycle models (Friedlingstein *et al.*, 2006; Hurtt *et al.*, 2010).

Forest cover and forest structure provide additional important feedbacks on biophysical properties and processes like albedo and evapotranspiration. Thus, improving our knowledge about the state of the world's forests is also important for understanding their influence on energy and water fluxes. Beside their ecological importance, forests are also of great social, economic (Bonan, 2008) and even political value in terms of the Reducing Emissions from Deforestation and Degradation (REDD) scheme (UN-REDD, 2011). Despite their relevance, forests are at risk due to deforestation and degradation processes. Although reforestation is expected to have exceeded deforestation in boreal and temperate forests in the period between 1990 and 2010, logging, fires and insects can have a significant impact in these biomes at regional scales (FAO, 2010).

Current estimates of the carbon stock for boreal and temperate forests are usually based upon upscaling of often sparse forest inventory data to national estimates. Such approaches involve a poor spatial resolution and high remaining uncertainty (Boudreau *et al.*, 2008). Previous studies show important divergences in estimated carbon stocks and densities of temperate and boreal forests (e.g. Saugier *et al.*, 2001; Pan *et al.*, 2011). Although there are discrepancies in the methods used for estimating biomass, and in the forest area and biomass compartments considered, these large differences highlight the need to improve our knowledge of the current state of non-tropical forests.

As forest inventories are always limited, especially in remote areas, remote sensing can serve as a very useful tool for monitoring the state and also the dynamics of forest ecosystems. While biomass maps based on remote sensing data recently became available for the tropics (Saatchi *et al.*, 2011; Baccini *et al.*, 2012), spatially explicit datasets on forest carbon stocks in the Northern Hemisphere have been rare and inconsistent up to now. Remote sensing has shown the potential to overcome this shortcoming and biomass has already been successfully mapped using light detection and ranging (LiDAR; e.g. Lefsky *et al.*, 2002; Boudreau *et al.*, 2008) and synthetic aperture radar (SAR; e.g. Ranson *et al.*, 1997; Wagner *et al.*, 2003; Neumann *et al.*, 2012) data. However, these studies either do not cover the whole extent of temperate and boreal forests in a single product, rely on using classifications with an early biomass saturation and/or are highly dependent on inventory data.

The availability of extensive observations by the Envisat Advanced Synthetic Aperture Radar (ASAR) has boosted the development of an algorithm to retrieve forest growing stock volume (GSV) (Santoro *et al.*, 2011, 2013). The major innovation of this retrieval algorithm, referred to as the BIOMASAR algorithm, is that it does not require reference data to calibrate the model linking the remote sensing observation with the output variable, i.e. the GSV. Recently, a dataset of GSV estimates covering the Northern Hemisphere between 30° N and 80° N, and thus including the boreal and temperate forests of North America, Europe and Asia, was generated with the BIOMASAR algorithm at a spatial resolution of 0.01° (Santoro *et al.*, in prep.). While forestry and remote sensing scientists tend to quantify 'biomass' in terms of GSV, scientists working on the carbon cycle and climate modelling, as well as national carbon monitoring systems (involved in REDD), require information on how much carbon is stored in vegetation expressed in mass units, and comprising in addition estimates of carbon in other tree compartments such as branches and roots. This allows for comparison with the carbon pools usually implemented in dynamic global vegetation models (DGVMs; e.g. Moorcroft *et al.*, 2001; Beer *et al.*, 2006; Randerson *et al.*, 2009) on the one hand and for assessment of national forest resources (e.g. DeFries *et al.*, 2002; Grainger, 2009) on the other.

Many studies have inferred biomass from GSV by applying so-called biomass expansion factors, which were empirically derived for a certain species or region (e.g. Somogyi *et al.*, 2008; Teobaldelli *et al.*, 2009; Guo *et al.*, 2010). In contrast, this study intends to derive biomass from GSV using information on wood density and the allometric relation between biomass compartments. At the same time, these relations should be consistently applicable over the whole study area. This approach allows for a division between biomass compartments (stem, branches, roots, foliage), which can provide useful information for applications requiring such detailed data.

The aims for this study are (1): to infer a consistent forest carbon map from recently available remote sensing GSV data, (2) to provide spatially explicit uncertainty estimates to the biomass map, (3) to estimate the total carbon stocks in Northern Hemisphere boreal and temperate forests, (4) to evaluate the derived product against independent datasets, and finally (5) to demonstrate the potential of multitemporal Envisat ASAR data to consistently map biomass at a moderate resolution covering large areas.

MATERIALS AND METHODS

GSV data

This study is based on GSV estimates obtained with the BIOMASAR algorithm from large numbers of observations by the ASAR instrument on board the Envisat satellite (Santoro *et al.*, 2011). Forest GSV refers to the volume of tree stems per unit area and is measured in $m^3\ ha^{-1}$. The GSV estimated from the SAR data is determined by (1) the wavelength of the ASAR instrument (5.6 cm) and (2) the structural and dielectric properties of the forest. Objects with a size smaller than the wavelength are transparent to ASAR; similarly, objects with frozen water are transparent. By combining in a weighted approach individual GSV estimates from primarily winter-time ASAR data, the GSV estimation procedure extracts the maximum in terms of signal related to GSV in the radar data (Santoro *et al.*, 2011). Stumps are accounted for in the ASAR GSV estimate as long as they are seen by ASAR, i.e. their size is larger than the

wavelength and they are standing. GSV estimates might also contain a necromass component if this is directly sensed by the radar. However, these aspects have not been quantified so far.

Spatially explicit GSV data with a resolution of 0.01° were obtained for North America, Europe and Asia covering the latitudes between 30° N and 80° N. The multitemporal SAR dataset was acquired between October 2009 and February 2011, thus containing information on the state of the vegetation structure in the year 2010. GSV was mapped without saturation up to 300 m^3 ha^{-1}. Above this level the retrieved GSV was characterized by a tendency to saturate, i.e. increasing underestimation for increasing GSV (Santoro *et al.*, unpublished data). However, less than 1% of the pixels in the study area had a GSV above this value. The uncertainty of GSV estimates was quantified to be 10% (Santoro *et al.*, 2011). The BIOMASAR algorithm retrieves GSV regardless of the vegetation type. To ensure that the biomass estimates reported here correspond to a forest type of vegetation, non-forested areas were masked out beforehand according to the GLC2000 land-use/land-cover map (JRC, 2003; see Appendix S1 in Supporting Information).

Additional datasets

In addition to GSV, the Global Wood Density Database (Chave *et al.*, 2009; Zanne *et al.*, 2009) and the JRC GHG-AFOLU Biomass Compartment Database (JRC, 2009) were used in this study. While the Global Wood Density Database contains information on wood density, the JRC Biomass Compartment Database includes measurements of the absolute amount of biomass in different compartments, both over a wide range of species and sufficiently covering the study area. The Global Wood Density Database consists of more than 16,000 entries, covering more than 8000 tree species. The JRC Biomass Compartment Database also gives additional information on latitude/longitude, tree age, diameter, height and density amongst other things.

As there is no detailed tree species map available covering the whole study area, information contained in those databases had to be aggregated to the level of leaf types (broadleaf, needleleaf deciduous, needleleaf evergreen forest). GLC2000 could be further used to distinguish between leaf types. GLC2000 assigns one of 22 different land-cover classes to each pixel. These classes were summarized to broadleaf, needleleaf deciduous, needleleaf evergreen, mixed forest and non-forest (for details see Appendix S1). GLC2000 was reprojected using nearest neighbour resampling to 0.01° in order to match the resolution of the GSV map.

Derivation of total forest carbon from GSV

In a first step, stem biomass (SB) was derived from GSV using information on wood density (WD) from the Global Wood Density Database (Fig. 1) as follows:

$$SB = GSV \times WD. \quad (1)$$

All the entries for different tree species contained in the database were summarized to tree genera and leaf types. In the absence of a global tree species map, no weighting according to the occurrence of tree species could be implemented. Investigations concentrated on the most common genera in boreal and temperate forests, including *Abies*, *Acer*, *Alnus*, *Betula*, *Fagus*, *Fraxinus*, *Larix*, *Picea*, *Pinus*, *Populus*, *Quercus*, *Tilia* and *Tsuga*. For each pixel of the GSV map stem biomass was calculated following equation (1). Mean wood density per leaf type has been applied according to the leaf type distribution derived from the GLC2000 land-cover map.

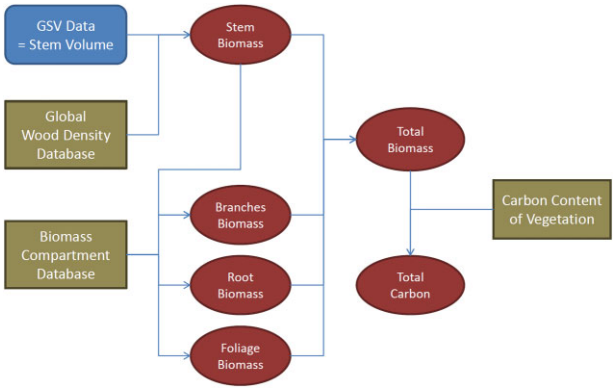

Figure 1 Processing algorithm.

In a second step, allometric relationships at leaf type level between stem biomass and the other required biomass compartments (BC; including branches, foliage, roots) were derived by fitting root functions to the Biomass Compartment Database. Nonlinear models of the following form were fitted using generalized least square regression (Pinheiro & Bates, 2000):

$$BC = a \times SB^{1/b}. \quad (2)$$

The model form is similar to the allometric relationships used by Zianis *et al.* (2005) and Wutzler *et al.* (2008), although we used stem biomass instead of tree diameter as a predictor. Branch, root and foliage biomass were calculated in this manner. These relationships were applied to the stem biomass map leading to maps of the other biomass compartments. The coefficients a and b in equation (2) were also derived for each leaf type. Then, the GLC2000 land-cover map was applied again to estimate biomass compartments for the different leaf types. *Abies*, *Alnus*, *Betula*, *Fagus*, *Larix*, *Picea*, *Pinus*, *Populus*, *Quercus* and *Tsuga* could be included in this analysis. Unfortunately, for *Acer*, *Fraxinus* and *Tilia* there was not sufficient information (at least 10 database entries) on root biomass available in the database.

Finally, total biomass (TB) was inferred as the sum of the biomass compartments stem, branches (BB), root (RB) and foliage biomass (FB):

$$TB = SB + BB + RB + FB. \quad (3)$$

The carbon content in vegetation varies between leaf type and biomes (Thomas & Martin, 2012); however, variations between plant tissues are of minor importance. This was taken into account here:

$$TC = 0.488TB \quad (4)$$

for temperate/boreal broadleaf tree species and

$$TC = 0.508TB \quad (5)$$

for temperate/boreal needleleaf tree species.

Uncertainty analysis

In addition to the total carbon density map, an uncertainty estimate was derived for each pixel. Here we refer to uncertainty in terms of the standard deviation of the biomass value. All the steps of the processing algorithm contribute to the overall uncertainty. Factors adding uncertainty to the final product include: (1) uncertainty of the BIOMASAR GSV estimates; (2) uncertainty of GLC2000 land-use/land-cover classification; (3) uncertainty of wood density data; (4) uncertainty of biomass compartment data; (5) uncertainty of the carbon content in vegetation.

The relative error of GSV estimates related to the retrieval algorithm was quantified by Santoro *et al.* (2011) to be on average 10%. The uncertainty of GLC2000 land cover could not be accounted for in this analysis. It is assumed to slightly affect the spatial distribution of uncertainties, but to have only a minor effect on their overall range. The land-cover classification potentially introduces uncertainty by applying a wood density or an allometric relation for the wrong leaf type. The standard deviation of wood density for different leaf types, containing its variance between species, could be used to quantify its uncertainty. The uncertainty introduced by the relationship between biomass compartments, which is caused by the variation of allometric functions within leaf types, was estimated from the variance of residuals of the model fit. It was estimated by applying a generalized model (Pinheiro & Bates, 2000; Zuur *et al.*, 2009). This kind of model allowed an increase of the variance of residuals with increasing covariate, in this case the stem biomass. Hence an increasing uncertainty in branch, root and foliage biomass could be modelled with increasing stem biomass. The uncertainty of the carbon content of vegetation was considered negligible compared with the magnitude of the other uncertainties.

Error propagation was implemented following Taylor (1997). We applied a Gaussian error propagation (GEP) approach. Its use in ecological studies has been demonstrated by Lo (2005) for a similar example. It was found to be especially beneficial when implying step-by-step calculations or different scales, both of which are relevant to this study.

Uncertainty of stem biomass (u_{SB}) can be calculated from the relative error of GSV (u_{GSV} = 10% GSV) and the standard deviation of wood density (u_{WD}). These uncertainties can be assumed to be independent and random:

$$u_{SB} = \sqrt{\left(\frac{dSB}{dGSV}\cdot u_{GSV}\right)^2 + \left(\frac{dSB}{dWD}\cdot u_{WD}\right)^2} = \sqrt{(WD\cdot u_{GSV})^2 + (GSV\cdot u_{WD})^2} \quad (6)$$

Here dSB/dGSV denotes the partial derivative of SB with respect to GSV. The uncertainty of branches biomass (u_{BB}) for given stem biomass consists of the propagated uncertainty of stem biomass and the uncertainty of the fitted relationship between those two variables ($u_{BB=f(SB)}$, cf. Taylor, 1997, p. 190), which is caused by the uncertainty of the Biomass Compartment Database. Again, these uncertainties can be assumed to be independent and random:

$$u_{BB} = \sqrt{\left(\frac{dBB}{dSB}\cdot u_{SB}\right)^2 + u^2_{BB=f(SB)}} = \sqrt{\left(\frac{a}{b}\cdot SB^{\frac{1}{b}-1}\cdot u_{SB}\right)^2 + u^2_{BB=f(SB)}} \quad (7)$$

The derivatives are evaluated at given stem biomass and estimated model parameters. The uncertainty of the allometric function can be derived from the generalized model. We are interested in the uncertainty introduced by the influence of species, climate, tree age and other possible factors on this allometric relation. The variance of the residuals is expressed in dependence of the residual standard error (RSE) and rising with the power of the absolute value of the covariate (SB). The parameter δ is fitted by the model (Pinheiro & Bates, 2000; Zuur *et al.*, 2009):

$$u^2_{BB=f(SB)} = RSE^2 \times |SB|^{2\delta} \quad (8)$$

The uncertainty of root (u_{RB}) and foliage (u_{FB}) biomass can be derived in the same way.

As the uncertainties of the biomass compartments cannot be considered to be independent (they are all calculated out of stem biomass; i.e. if the uncertainty in stem biomass increases, the uncertainty in the other biomass compartments will also increase), the uncertainty in their sum (u_{TB}) has to be calculated as the sum of the original uncertainties:

$$u_{TB} = u_{SB} + u_{BB} + u_{RB} + u_{FB}. \quad (9)$$

Finally, the uncertainty of total biomass was propagated in order to derive the uncertainty of total carbon, assuming negligible uncertainty of carbon content:

$$u_{TC} = \frac{dTC}{dTB}u_{TB} = 0.488u_{TB} \quad (10)$$

for temperate/boreal broadleaf tree species and

$$u_{TC} = \frac{dTC}{dTB}u_{TB} = 0.508u_{TB} \quad (11)$$

for temperate/boreal needleleaf tree species.

Evaluation

The carbon map we produced was evaluated against different independent datasets, covering an exhaustive range of ecosystems and forest structures. For intercomparison, Russian forest enterprise data (Shvidenko *et al.*, 2010; Schepaschenko *et al.*,

2011), the United States National Biomass and Carbon Dataset for the year 2000 (NBCD2000; Kellndorfer *et al.*, 2010; Kellndorfer *et al.*, 2012) and European national statistics (EFI, 2005) were used. The intercomparison was implemented at a regional level (Russian forest enterprises, US counties, European countries) to ensure that the biomass values in the two datasets refer to the forest structure, i.e. are of the same scale.

The Russian land-cover dataset produced by the International Institute for Applied Systems Analysis (IIASA; Shvidenko *et al.*, 2010; Schepaschenko *et al.*, 2011) is based on integration of forest inventory data and other relevant information. The dataset contains detailed forest characteristics (species composition, age, GSV, biomass etc.) at 1-km resolution. Intercomparison was performed for approximately 1600 forest enterprises with an average area of 9132.3 km^2, ranging from 2.8 to 550,074.0 km^2. While forest enterprises are usually small in densely populated territories in European Russia, they cover very large areas in remote territories of Siberia.

NBCD2000 (Kellndorfer *et al.*, 2012) was produced by the Woods Hole Research Center (WHRC) and can be seen as a benchmark map covering the conterminous United States. Combining United States Department of Agriculture (USDA) Forest Service Forest Inventory and Analysis (FIA; USDA, 2012) and remote sensing data [interferometric SAR (InSAR) data from the Shuttle Radar Topography Mission (SRTM) and optical Landsat data], a high-resolution (30 m) raster dataset of aboveground wood carbon was derived (Kellndorfer *et al.*, 2010, 2012). Aggregated biomass values could be compared for more than 3000 counties with an average area of 2405.7 km^2, ranging from 0.8 to 52,109.4 km^2. The comparison at the level of forest enterprises, counties or countries ensures a comparison to original forest inventory data and is not affected by the spatial variability introduced by other remote sensing data into the reference datasets.

Estimation of boreal and temperate forest carbon stock and density

Based on the new total carbon density map, boreal and temperate forest carbon stock and carbon density were estimated across three continents – North America, Europe and Asia. Biomes were extracted according to Olson *et al.* (2001), including boreal forests (BFT), temperate broadleaf/mixed forests (TBMF) and temperate conifer forests (TCF). Continental boundaries were defined according to ESRI (2008). The land-cover map GLC2000 was used as a forest mask in order to specify forest area. GLC2000 considers a pixel containing more than 15% tree cover as forest (JRC, 2003). When deriving biomass estimates at a coarser spatial scale, the actual area of each grid cell was explicitly taken into account, assuming the earth to be a perfect sphere. The carbon stock and its corresponding uncertainty of biomes and continents were calculated as the sum of the absolute biomass and uncertainties of the corresponding pixel values, respectively. In order to derive the carbon density and its uncertainty per biome and continent, the carbon stock and its uncertainty were divided by the covered area.

Table 1 Wood density mean and standard deviation obtained from the Global Wood Density Database for different leaf types.

Forest leaf type	Broadleaf	Needleleaf deciduous	Needleleaf evergreen
Mean wood density (g cm^{-3})	0.570	0.464	0.411
Standard deviation of wood density (g cm^{-3})	0.150	0.057	0.066

RESULTS AND DISCUSSION

Wood density

The mean values and standard deviations of wood density for different leaf types are summarized in Table 1. Corresponding boxplots show the median values and quartiles not only across leaf types but also in more detail across tree genera (Fig. 2). As the differences between mean and median values are negligible, the mean values can be considered to describe the distributions of wood density sufficiently well. Thus, they were used to calculate stem biomass following equation (1). When summarized to leaf types, the wood density of broadleaf trees in particular varies considerably between tree species. In this processing step, the uncertainty introduced by the Global Wood Density Database is relatively large for broadleaf trees. In terms of their mean value, broadleaf trees have the highest wood density and thus a higher biomass per volume, followed by needleleaf deciduous and needleleaf evergreen trees.

Allometric relationships

The allometric relationships between branch, root and foliage biomass to stem biomass were found to be best modelled as a root function (Fig. 3). While an increasing stem biomass is able to support the growth of more branches and also leaves, at the same time more biomass has to be allocated to roots in order to supply water and nutrients for increasing maintenance and growth needs. These findings are consistent with the pipe model (Shinozaki *et al.*, 1964). Increasing competition for resources with increasing stand biomass is responsible for the nonlinearity of the relationship. The database contained trees with a stem biomass up to about 400 t ha^{-1}. While broadleaf trees were found to be able to support higher branch biomass, needleleaf evergreen trees were found to have higher foliage biomass compared with the other leaf types. However, at a 95% confidence interval, these findings were not significant, except a significantly higher multiplier in the allometric relation between foliage and stem biomass for needleleaf evergreen trees compared with broadleaf trees. The modelled relationship of root biomass to stem biomass was not significantly different between leaf types. Relative uncertainty introduced in this processing step is highest for inferring foliage biomass from stem biomass, especially for needleleaf deciduous trees with low stem biomass values.

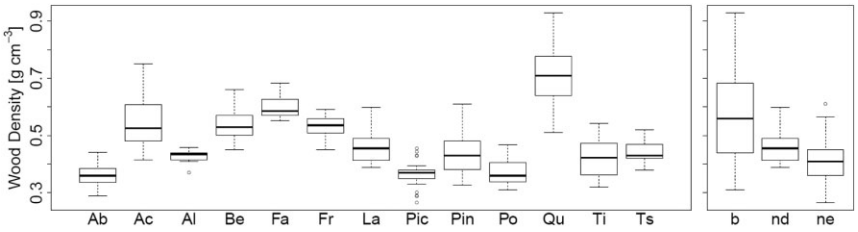

Figure 2 Variance in wood density (g cm^{-3}) measurements contained in the Global Wood Density Database across tree genera (left: Ab, *Abies*; Ac, *Acer*; Al, *Alnus*; Be, *Betula*; Fa, *Fagus*; Fr, *Fraxinus*; La, *Larix*; Pic, *Picea*; Pin, *Pinus*; Po, *Populus*; Qu, *Quercus*; Ti, *Tilia*; Ts, *Tsuga*) and leaf types (right: b, broadleaf; nd, needleleaf deciduous; ne, needleleaf evergreen). The box–whisker plots show the median and the interquartile range of values. The whiskers extend up to the most extreme data point which is no more than 1.5 times the interquartile range away from the box. Outliers are drawn as circles.

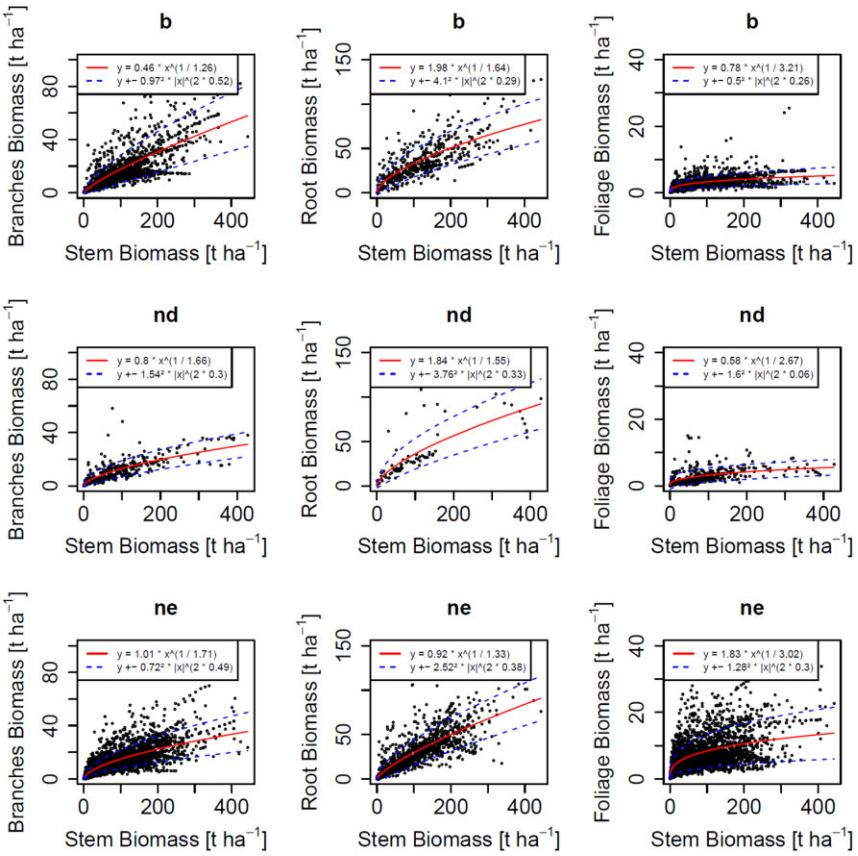

Figure 3 Fitted allometric relationships between stem, branch, root and foliage biomass (t ha^{-1}) using the Biomass Compartment Database [b, broadleaf; nd, needleleaf deciduous; ne, needleleaf evergreen; central solid line, functional relationship; upper and lower bound (dashed), uncertainty bound (standard deviation of the residuals)].

Carbon density map

Most of the forests with the highest carbon content per area (> 8 kg C m^{-2}) are situated along the Rocky Mountains in north-west Canada and the USA, the European mountains (both mostly temperate coniferous forest), European Russia, southern central Siberia (temperate broadleaf and mixed forests, southern boreal forests) and Japan (mostly temperate broadleaf and mixed forests; Fig. 4). In the boreal zone, forest carbon decreases to the north along a latitudinal gradient. The spatial patterns give information on potential carbon loss due to disturbances or potential availability of wood to humans. Corresponding relative uncertainty is most often between 20 and 40%, especially in the high-biomass areas. The lowest relative uncertainties are estimated in the high-biomass areas of north-west Canada and the USA, central Siberia, most European mountain ranges and Japan. The relative uncertainty of this modelling approach increases in the northern taiga, where there is very low biomass.

The individual biomass compartment maps are presented in detail in Appendix S2. The differences in spatial patterns follow the distributions of leaf types in GLC2000 and can be explained by the differences between leaf types in modelled compartment relationships (Fig. 3). The relative uncertainty of stem carbon (Appendix S2) is below 20% in most areas, except for broadleaf trees where the high variation in wood density causes higher

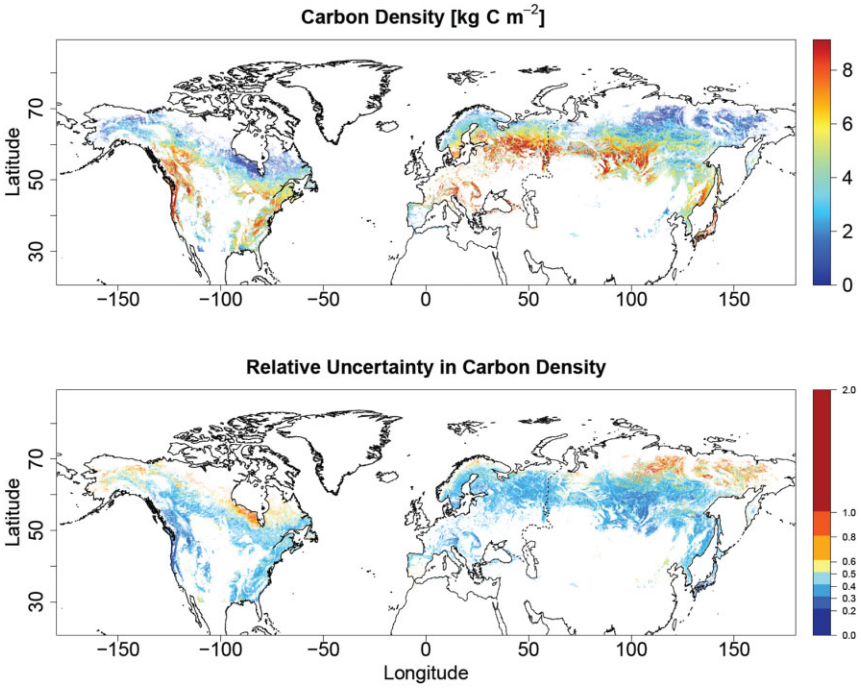

Figure 4 Spatial distribution of total forest carbon density (tree stems + branches + roots + foliage) in Northern Hemisphere boreal and temperate forests and its corresponding relative uncertainty (a value of 1 means 100% uncertainty). Non-forest is masked out according to the GLC2000 land-use/land-cover map (JRC, 2003). The dashed black line indicates the boundary between Europe and Asia (data from ESRI, 2008) used for the estimation of continental carbon stocks in this study.

uncertainties. Modelling of branch, and particularly root and foliage carbon, introduces additional uncertainty (Appendix S2), which is highest (in relative terms) in low-biomass areas (mostly the northern taiga). But as the total carbon map is dominated by stem biomass, while the other compartments account only for a small proportion of total carbon, the overall relative uncertainty of the final map (Fig. 4) is within a very satisfactory range.

For Russia, the estimated carbon density at forest enterprise level agrees well with IIASA data ($r^2 = 0.78$, RMSE = 1.13 kg C m^{-2}, Fig. 5a). In an additional investigation no significant differences in this relationship were found for different bioclimatic zones in Russia (Appendix S3). For the USA, the comparison of aggregated values at county level shows strong agreement with the WHRC NBCD 2000 dataset ($r^2 = 0.90$, RMSE = 0.54 kg C m^{-2}, Fig. 5b). For European countries, evaluation results are comparable ($r^2 = 0.70$, RMSE = 0.87 kg C m^{-2}, Fig. 5c). While there is no systematic error apparent from the intercomparison in Russia, our product might slightly underestimate high carbon densities, as can be seen from the evaluation results for US and European data.

Boreal and temperate forest carbon stock and carbon density

In 2010, the boreal and temperate forests of the Northern Hemisphere (30 to 80° N) stored about 79.8 ± 29.9 Pg C (Table 2) and their mean carbon density was 4.76 ± 1.78 kg C m^{-2} of forest area (Table 3). Most of the forest carbon in the Northern Hemisphere is stored in BFT (40.7 ± 15.7 Pg C), while TBMF and TCF account for 24.5 ± 9.4 Pg C and 14.5 ± 4.8 Pg C, respectively (Table 2). In terms of carbon density, 6.21 ± 2.07 kg C m^{-2} are retained in TCF and 5.80 ± 2.21 kg C m^{-2} in TBMF, whereas we found a mean carbon density of 4.00 ± 1.54 kg C m^{-2} in BFT

Table 2 Estimated mean and uncertainty of total forest carbon for North America, Europe and Asia across three different biomes. Uncertainty denotes the aggregated uncertainty (i.e. standard deviation) of each pixel belonging to the specific biome and continent.

Total forest carbon (Pg C)	North America	Europe	Asia	Sum of three continents
TBMF	9.7 ± 3.8	8.6 ± 3.1	6.2 ± 2.4	24.5 ± 9.4
TCF	10.1 ± 3.3	1.5 ± 0.5	2.9 ± 1.1	14.5 ± 4.8
BFT	8.9 ± 3.7	9.8 ± 3.6	22.1 ± 8.3	40.7 ± 15.7
Sum of three biomes	28.7 ± 10.8	19.9 ± 7.3	31.2 ± 11.8	79.8 ± 29.9

TBMF, temperate broadleaf and mixed forests; TCF, temperate conifer forests; BFT, boreal forests/taiga.

Table 3 Estimated mean and uncertainty of carbon density for North America, Europe and Asia across three different biomes. Uncertainty denotes the aggregated uncertainty (i.e. standard deviation) of each pixel belonging to the specific biome and continent.

Carbon density (kg C m^{-2} forest)	North America	Europe	Asia	Mean of three continents
TBMF	5.42 ± 2.14	6.70 ± 2.46	5.38 ± 2.05	5.80 ± 2.21
TCF	6.42 ± 2.07	7.60 ± 2.62	5.13 ± 1.86	6.21 ± 2.07
BFT	2.99 ± 1.26	5.47 ± 2.04	4.07 ± 1.53	4.00 ± 1.54
Mean of three biomes	4.53 ± 1.71	6.08 ± 2.24	4.36 ± 1.64	4.76 ± 1.78

TBMF, temperate broadleaf and mixed forests; TCF, temperate conifer forests; BFT, boreal forests/taiga.

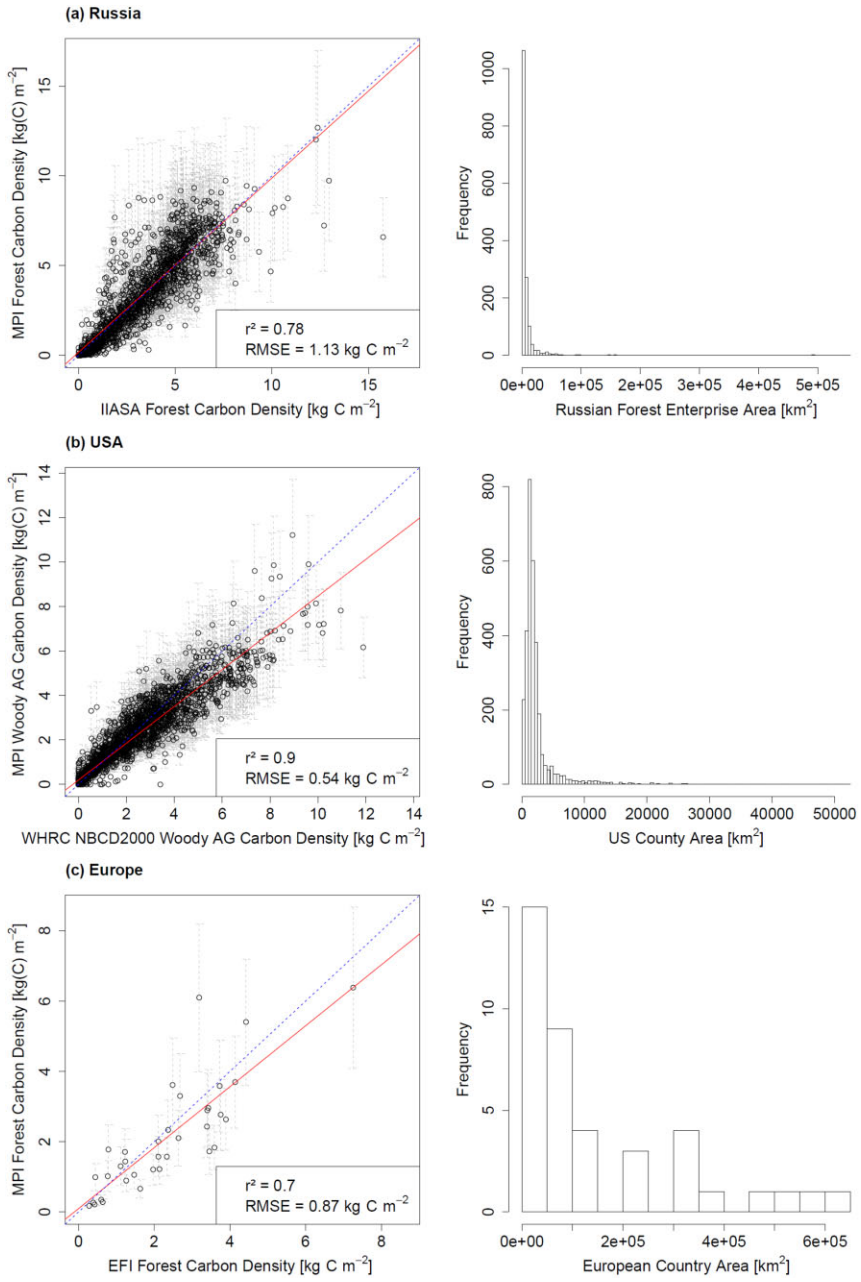

Figure 5 Intercomparison of carbon density data from this study (MPI) and (a) IIASA forest enterprise, (b) WHRC NBCD2000 US county, and (c) EFI European country carbon density data. The dotted line is the 1-to-1 line. The solid line is the linear regression line. Please note: here carbon density is calculated per total (enterprise/county/country) area, not per forest area, due to differences in the estimated forest area between products. Corresponding histograms show the spatial scale at which evaluation took place.

(Table 3). The uncertainty of these estimates is the sum of the uncertainties of all 0.01° pixels and is within the range of 30–40%.

Forest biome carbon stock and density values were also obtained more detailed for North America, Europe and Asia (see Tables 2 & 3 and Fig. 6). Asian BFT account for the largest carbon stock within the investigated biomes. Concerning carbon density, TBMF were found to have a higher carbon density than TCF in Asia, in contrast to the other two continents. European forests exhibit a higher carbon density across all the three biomes compared with North America and Asia. Due to the conservative approach of estimating uncertainty implemented in this study, many of these findings are not significant at the 95% confidence interval. However, some of the reported results are significant. Carbon stocks (Table 2) in TCF are significantly smaller in Europe and Asia than in North America. On the other hand, carbon stocks in BFT are significantly higher in Asia than in Europe and North America. In Europe, there is significantly less carbon stored in TCF than in TBMF and BFT, while in Asia carbon stocks were found to be significantly higher in BFT than in TBMF and TCF. Carbon density (Table 3) is significantly higher in European versus North American BFT. In North America, carbon density was found to be significantly higher in TBMF and TCF than in BFT.

While European forest carbon stocks are relatively small compared with those of the other continents, the carbon density is higher in Europe across all the three biomes compared with North America and Asia (Fig. 6, see also Tables 2 & 3). These patterns are also visible in Fig. 7, which shows carbon density per

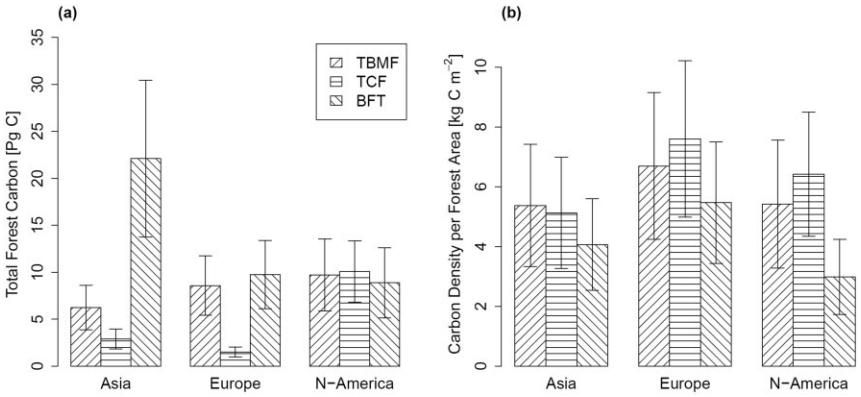

Figure 6 (a) Total carbon stored in Northern Hemisphere forests (TBMF, temperate broadleaf and mixed forests; TCF, temperate conifer forests; BFT, boreal forests/taiga) and (b) their corresponding carbon density.

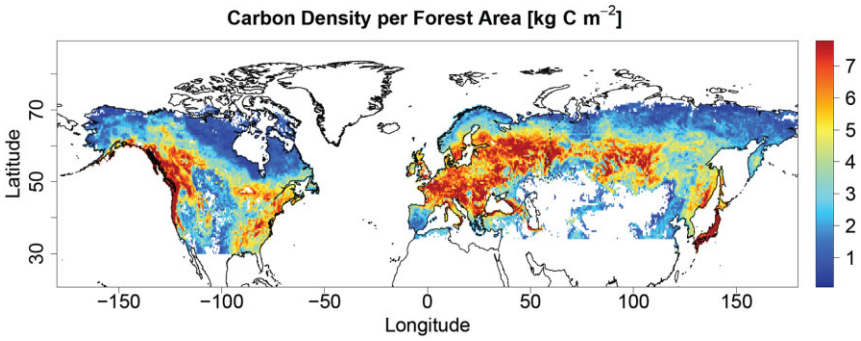

Figure 7 Spatial distribution of carbon density per forest area in Northern Hemisphere boreal and temperate forests (aggregated to 0.5° resolution). The dashed black line indicates the boundary between Europe and Asia (data from ESRI, 2008) used for the estimation of continental carbon stocks in this study.

Table 4 Total forest carbon values reported in other studies. Pan *et al.* (2011) distinguished between continents and biomes. Goodale *et al.* (2002) and Liski *et al.* (2003) distinguished between continents only. Saugier *et al.* (2001) distinguished between biomes only.

Other studies	Total forest carbon (Pg C)	North America	Europe	Asia	Sum of three continents	Saugier *et al.* (2001)§
Pan *et al.* (2011)*	TBMF + TCF	**19.4**	**10.5**	**8.3**	38.2	139
	BFT	**14.0**	**12.1**	**27.9**	53.9	57
	Sum of three biomes	**33.4**	**22.6**	**36.2**	92.1	196
Goodale *et al.* (2002)†	Sum of three biomes	31.3	52.2		83.5	
Liski *et al.* (2003)‡	Sum of three biomes	31	49		80	

TBMF, temperate broadleaf and mixed forests; TCF, temperate conifer forests; BFT, boreal forests/taiga.
*Forest total living biomass from 2007; understorey vegetation may be excluded if very small compared with total biomass; excluding Australia, New Zealand and 'other countries'.
†Live vegetation from 1990; including understorey vegetation.
‡Woody biomass on forest and other wooded land in temperate and boreal forests; including dead trees; including shrubs and bushes; from early/mid 1990s; China, Korea and Japan excluded.
§Carbon in living phytomass; including understorey vegetation; based on different studies.

forest area aggregated to a regional scale (0.5° pixel size). Carbon stocks per area of forest are estimated to be high in central Europe, for example (Fig. 7), while relative to total land the carbon density is small (Fig. 4) since the European landscape is dominated by agricultural areas. Average biomass density is higher in Europe, probably due to the influence of favourable climatic conditions, forest management activities and protected areas. Such information is important, for example for a comparison with process-oriented ecosystem models, such as DGVMs, which are often operated at coarser spatial resolutions like 0.5°.

The obtained forest carbon stock and density values were compared against estimates reported in the literature (Tables 4 & 5), although differences in the method for estimating biomass, the forest area and biomass compartments considered and in the time of investigation limit a direct comparison with other studies. The inclusion of understorey and green forest floor vegetation in literature values in particular might contribute substantially to some disagreements with our reported values, particularly in boreal forests (Schepaschenko *et al.*, 1998; Shvidenko *et al.*, 2007). Furthermore, differences in the

Table 5 Carbon density values calculated from other studies. Pan *et al.* (2011) distinguished between continents and biomes. Goodale *et al.* (2002) and Liski *et al.* (2003) distinguished between continents only. Saugier *et al.* (2001) distinguished between biomes only.

Other studies	Carbon density (kg C m^{-2} forest)	North America	Europe	Asia	Mean of three continents	Saugier *et al.* (2001)§
Pan *et al.* (2011)*	TBMF + TCF	**7.55**	**7.27**	**4.47**	6.51	13.35
	BFT	**6.10**	**5.28**	**4.12**	4.76	4.15
	Mean of three biomes	**6.87**	**6.05**	**4.20**	5.35	8.13
Goodale *et al.* (2002)†	Mean of three biomes	4.46	3.88		4.07	
Liski *et al.* (2003)‡	Mean of three biomes	4.3	4.3		4.3	

TBMF, temperate broadleaf and mixed forests; TCF, temperate conifer forests; BFT, boreal forests/taiga.
*Forest total living biomass and forest area data from 2007; understorey vegetation may be excluded if very small compared with total biomass; excluding Australia, New Zealand and 'other countries'.
†Live vegetation and total forest and woodland area from 1990; including understorey vegetation.
‡Woody biomass on forest and other wooded land in temperate and boreal forests; including dead trees; including shrubs and bushes; from early/mid 1990s; China, Korea and Japan excluded.
§Carbon in living phytomass; including understorey vegetation; based on different studies; using biome area instead of forest area.

definition of GSV between forest inventory and Envisat ASAR data, primarily concerning the inclusion of trees of certain diameters, stumps and necromass, can potentially lead to a bias in the estimated biomass. However, the validation of remote sensing-based biomass against inventory-based estimates showed no clear bias (Santoro *et al.*, 2011). Therefore, we assume the effects of GSV definition to be small compared with other sources of uncertainty. The shift in time between our product and other studies can further contribute to differences, since forest carbon stocks might have been affected significantly, for example by fires, insects (Kurz *et al.*, 2008) or climate change (Allen *et al.*, 2010), in the meantime.

Estimated temperate forest carbon stocks agree well with recently published results by Pan *et al.* (2011), who used a different biomass estimation method based mainly on forest inventory data. The value reported by Saugier *et al.* (2001) for temperate forests seems to be far too high in light of our study. The estimated value for boreal forests is a bit lower than those of Pan *et al.* (2011) and Saugier *et al.* (2001), but at least the value from Pan *et al.* (2011) is within the range of uncertainty of this study. Carbon stocks derived by Goodale *et al.* (2002) and Liski *et al.* (2003) for North America and Eurasia were very close to the results of this study, and were well below the uncertainty margin.

We confirm higher carbon densities in temperate forests compared with boreal forests as already reported by Pan *et al.* (2011) and Saugier *et al.* (2001). Values estimated for boreal forests agree well with these studies; however Saugier *et al.* (2001) dramatically overestimate temperate forest carbon density. While all the densities stated by Pan *et al.* (2011) for European and Asian boreal and temperate forests are within the uncertainty of the values calculated in this study, Pan *et al.* (2011) reported much higher carbon densities in North America, especially for boreal forests. Carbon densities calculated by Goodale *et al.* (2002) and Liski *et al.* (2003) are close to our estimates in North America, but lower in Eurasia.

Outlook

A comparison of different sets of predictors for the modelling of allometric relationships has shown that the applied algorithm could be further improved by the availability of a consistent global tree species map. For example modelling of branch biomass out of stem biomass using a generalized additive model (GAM) (Hastie & Tibshirani, 1990; Wood, 2006; for a detailed description of methods see Appendix S4) was significantly improved in terms of adjusted R^2, root mean square error (RMSE) and Akaike's information criterion (AIC) (Akaike, 1974) when information on tree genus was taken into account (Fig. 8). In contrast, the approach used in this study could only make use of leaf type information in addition to the stem biomass. Results were similar for root and foliage biomass.

The Global Wood Density Database and the Biomass Compartment Database could be explored by tree genus and not by leaf type only. There is a need for a global tree species map comparable to the tree species map covering Europe available from JRC (Köble & Seufert, 2001). Further investigations could explore improvements in the derivation of a biomass map making use of such more detailed information. The consideration of different climate zones could further improve modelling of allometric relationships (Fig. 8). This would require more extensive and standardized measurements of biomass compartments, covering all important tree species across all the different climate zones. In contrast, tree age and tree density did not have much effect on GAM results. Such improvements would lead to a better biomass estimate and to a reduction in the uncertainty of the resulting total carbon map.

It should be noted that the uncertainty estimate given has to be interpreted as an upper bound. As discussed in Taylor (1997), the calculation of the uncertainty of the sum of biomass compartments as the sum of their uncertainties (equation 9) might also lead to an overestimation of the error in the case of dependent variables. A direct estimation of total biomass (as the sum

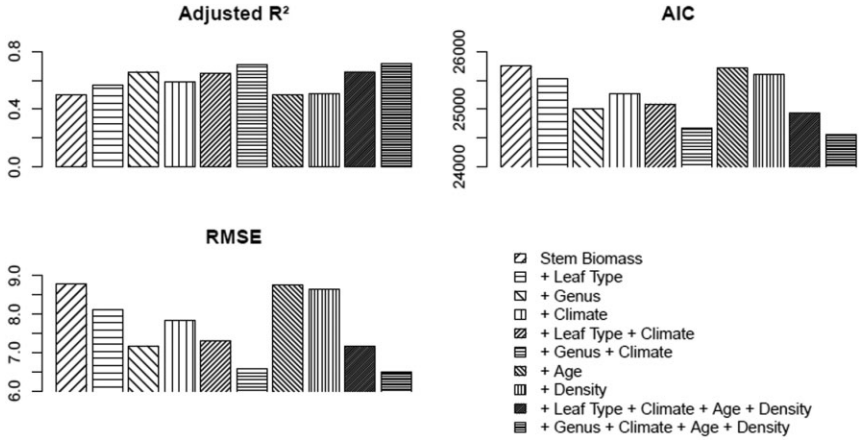

Figure 8 Generalized additive model (GAM) results modelling branch biomass using different sets of predictors (AIC, Akaike's information criterion; RMSE, root mean square error; for a detailed description of methods see Appendix S4).

of compartments) from stem biomass based on the Global Biomass Compartment Database would decrease the uncertainty estimate but lead to an inconsistency between the estimated biomass compartments and the total biomass. Nevertheless, the application of GEP allowed for a conservative uncertainty estimate over a large dataset. Its benefits for ecological studies have already been illustrated by Lo (2005). However, uncertainty estimation due to land cover and of the GSV product should be further improved.

Land-cover information is essential for our method of estimating the biomass at the 0.01° pixel size level since the leaf type determines the applied wood density and the parameters used for the allometric equation (equation 2). Therefore, assuming a pixel size of 0.01° × 0.01° to be covered by a single leaf type is a simplification in our study which we cannot avoid because the underlying GSV map also comes with this pixel size. At a higher level of aggregation, land-cover uncertainty directly translates into forest area uncertainty which is used to estimate total carbon stocks at a continental scale. In general, two types of uncertainty are important here: First, there is no information about forest area within a 0.01° land-cover pixel and second, misclassification leads to uncertainty in forest area at the continental scale. The subpixel uncertainty (first type) effect on carbon stock estimates is considered to be small. In case of a pixel that is classified as forest but in reality contains only minor tree coverage, the GSV estimate at the same scale will be also small. The effects of the second type of uncertainty are also considered to be small since forest misclassifications most often occur in heterogeneous landscapes (Mayaux *et al.*, 2006), where areas of sparse forests with low carbon stocks are usually situated. In this respect, using GLC2000 has the advantage of using a low threshold (15%) of tree cover for forest classification (JRC, 2003). In doing so, we make sure to include most forest areas.

The evaluation results indicate that the accuracy of the presented carbon density map is comparable to upscaled forest inventory data at a regional scale. This highlights the potential of remote sensing data to complement biomass inventories. Although Envisat ASAR data are not optimal and other SAR datasets exist that might lead to improved estimates, only Envisat ASAR data are available globally and are free to users. At a finer resolution of about 1 km, a direct comparison to other data remains problematic. Forest inventory data represent the stand scale and upscaling is also highly uncertain (Gibbs *et al.*, 2007; Saatchi *et al.*, 2007, 2011). Upscaling forest inventory data by high-resolution airborne LiDAR data is the most promising type of product for the evaluation of the small-scale variability of biomass (Patenaude *et al.*, 2004; Saatchi *et al.*, 2011). Such products are being processed currently and should be used in the near future. This will help to also understand if a resolution of 0.01° is also sufficient in spatially heterogeneous European forests or if a finer-scale mapping is required in patchy forest ecosystems.

CONCLUSION

In this study we have presented a biomass map originating from one consistent remote sensing and modelling approach, covering all the extratropical regions of the Northern Hemisphere in a single product with a moderate spatial resolution. This map, together with the spatially explicit quantification of its uncertainty, updates current estimates of the carbon currently stored in the forests of North America, Europe and Asia. Together with recent results of Saatchi *et al.* (2011) or Baccini *et al.* (2012), for example, it can be of great value for a wide range of users, spanning from global climate modellers to national carbon monitoring systems. Evaluation results have shown that this product can serve as a new benchmark regarding spatially explicit and consistent biomass and carbon mapping with moderate spatial resolution. The forest carbon density dataset (total carbon and single compartments) and its corresponding uncertainty are available at the BIOMASAR project website (http://www.biomasar.org) and at the GEOCARBON Data Portal (http://www.bgc-jena.mpg.de/geodb/projects/Home.php).

In the Northern Hemisphere, boreal and temperate forest carbon stocks were found to be almost equal in magnitude. Temperate forests have a higher carbon density than boreal forests. However, due to our conservative uncertainty estimate these findings could be proved to be significant only for North America. Despite higher carbon densities across boreal and tem-

perate forest biomes in Europe when compared with the other continents these are still within its confidence intervals. While our results confirm the temperate forest carbon given in Pan *et al.* (2011), there seems to be less carbon stored in boreal forests than previously estimated (Saugier *et al.*, 2001; Pan *et al.*, 2011), although such a comparison with other studies is problematic due to the different methods employed. We consider an earlier estimate of temperate forest biomass (Saugier *et al.*, 2001) to be unrealistically high. In the future, a regular repetition of consistent biomass estimation from remote sensing data may also help to improve our knowledge on disturbance, deforestation, degradation and regrowth processes in addition to the current state. The lack of continuity of most remote sensing missions is a disadvantage since it implies an additional cross-calibration step between GSV or biomass datasets obtained from different sensors and, therefore, retrieval approaches. The availability of a global tree species map as well as more comprehensive allometric biomass databases would further reduce the uncertainties of the results.

ACKNOWLEDGEMENTS

This study is supported by the European Space Agency (ESA) within the Support to Science Element (STSE) project BIOMASAR (ESRIN contract no. 21892/08/I-EC). The global land-cover map GLC2000 from the Joint Research Centre (JRC), the Global Wood Density Database and the JRC GHG-AFOLU Biomass Compartment Database contributed significantly to this work. For providing reference data on biomass, we want to acknowledge the United States National Biomass and Carbon Dataset for the year 2000 (NBCD2000, provided by Josef Kellndorfer) and the European Forest Institute (EFI).

REFERENCES

Akaike, H. (1974) A new look at the statistical model identification. *IEEE Transactions on Automatic Control*, **19**, 716–723.

Allen, C.D., Macalady, A.K., Chenchouni, H., Bachelet, D., McDowell, N., Vennetier, M., Kitzberger, T., Rigling, A., Breshears, D.B., Hogg, E.H., Gonzalez, P., Fensham, R., Zhang, Z., Castro, J., Demidova, N., Lim, J.-H., Allard, G., Running, S.W., Semerci, A. & Cobb, N. (2010) A global overview of drought and heat-induced tree mortality reveals emerging climate change risks for forests. *Forest Ecology and Management*, **259**, 660–684.

Baccini, A., Goetz, S.J., Walker, W.S., Laporte, N.T., Sun, M., Sulla-Menashe, D., Hackler, J., Beck, P.S.A., Dubayah, R., Friedl, M.A., Samanta, S. & Houghton, R. (2012) Estimated carbon dioxide emissions from tropical deforestation improved by carbon-density maps. *Nature Climate Change*, **2**, 182–185.

Beer, C., Lucht, W., Schmullius, C. & Shvidenko, A. (2006) Small net carbon dioxide uptake by Russian forests during 1981–1999. *Geophysical Research Letters*, **33**, L15403. doi:10.1029/2006GL026919.

Bellassen, V., Delbart, N., Le Maire, G., Luyssaert, S., Ciais, P. & Viovy, N. (2011) Potential knowledge gain in large-scale simulations of forest carbon fluxes from remotely sensed biomass and height. *Forest Ecology and Management*, **261**, 515–530.

Bonan, G.B. (2008) Forests and climate change: forcings, feedbacks, and the climate benefits of forests. *Science*, **320**, 1444–1449.

Boudreau, J., Nelson, R., Margolis, H., Beaudoin, A., Guindon, L. & Kimes, D. (2008) Regional aboveground forest biomass using airborne and spaceborne LiDAR in Québec. *Remote Sensing of Environment*, **112**, 3876–3890.

Chave, J., Coomes, D., Jansen, S., Lewis, S.L., Swenson, N.G. & Zanne, A.E. (2009) Towards a worldwide wood economics spectrum. *Ecology Letters*, **12**, 351–366.

DeFries, R.S., Houghton, R.A., Hansen, M.C., Field, C.B., Skole, D. & Townshend, J. (2002) Carbon emissions from tropical deforestation and regrowth based on satellite observations for the 1980s and 1990s. *Proceedings of the National Academy of Sciences USA*, **99**, 14256–14261.

Denman, K.L., Brasseur, G., Chidthaisong, A., Ciais, P., Cox, P.M., Dickinson, R.E., Hauglustaine, D., Heinze, C., Holland, E., Jacob, D., Lohmann, U., Ramachandran, S., da Silva Dias, P.L., Wofsy, S.C. & Zhang, X. (2007) Couplings between changes in the climate system and biogeochemistry. *Climate change 2007: the physical science basis. Contribution of Working Group I to the Fourth Assessment Report of the Intergovernmental Panel on Climate Change* (ed. by S. Solomon, D. Qin, M. Manning, Z. Chen, M. Marquis, K.B. Averyt, M. Tignor and H.L. Miller), 499–588. Cambridge University Press, Cambridge.

EFI (2005) *LTFRA database*. European Forest Institute. Available at: http://www.efi.int/portal/virtual_library/databases/ (accessed 8 June 2012).

ESRI (2008) *Continents shapefile*. Baruch Geoportal. Baruch College. City University of New York. Available at: <http://www.baruch.cuny.edu/geoportal/data/esri/esri_intl.htm (accessed 7 December 2012).

FAO (2010) *Global Forest Resources Assessment 2010. Main report*. FAO Forestry Paper 163. Food and Agriculture Organization, Rome.

Friedlingstein, P., Cox, P., Betts, R. *et al.* (2006) Climate–carbon cycle feedback analysis: results from the C(4)MIP model intercomparison. *Journal of Climate*, **19**, 3337–3353.

Gibbs, H.K., Brown, S., Niles, J.O. & Foley, J.A. (2007) Monitoring and estimating tropical forest carbon stocks: making REDD a reality. *Environmental Research Letters*, **2**, 045023. doi:10.1088/1748-9326/2/4/045023.

Goodale, C.L., Apps, M.J., Birdsey, R.A., Field, C.B., Heath, L.S., Houghton, R.A., Jenkins, J.C., Kohlmaier, G.H., Kurz, W., Liu, S.R., Nabuurs, G.J., Nilsson, S. & Shvidenko, A.Z. (2002) Forest carbon sinks in the Northern Hemisphere. *Ecological Applications*, **12**, 891–899.

Grainger, A. (2009) Towards a new global forest science. *International Forestry Review*, **11**, 126–133.

Guo, Z., Fang, J., Pan, Y. & Birdsey, R. (2010) Inventory-based estimates of forest biomass carbon stocks in China: a comparison of three methods. *Forest Ecology and Management*, **259**, 1225–1231.

Hastie, T.J. & Tibshirani, R.J. (1990) *Generalized additive models*. Chapman & Hall/CRC, Boca Raton, FL.

Hurtt, G.C., Fisk, J., Thomas, R.Q., Dubayah, R., Moorcroft, P.R. & Shugart, H.H. (2010) Linking models and data on vegetation structure. *Journal of Geophysical Research*, **115**, G00E10. doi:10.1029/2009JG000937.

JRC (2003) *Global Land Cover 2000 database*. European Commission. Joint Research Centre. Available at: http://bioval.jrc.ec.europa.eu/products/glc2000/glc2000.php (accessed 3 July 2012).

JRC (2009) *The Biomass Compartment Database of the GHG-AFOLU project of the European Commission*. Joint Research Centre. Available at: http://afoludata.jrc.ec.europa.eu/index.php/public_area/biomass_compartments (accessed 6 January 2012).

Kellndorfer, J., Walker, W., LaPoint, E. & Kirsch, K. (2010) Statistical fusion of LiDAR, InSAR, and optical remote sensing data for forest stand height characterization: a regional-scale method based on LVIS, SRTM, Landsat ETM+, and ancillary data sets. *Geophysical Research Letters*, **115**, G00E08.

Kellndorfer, J., Walker, W., LaPoint, E., Bishop, J., Cormier, T., Fiske, G., Hoppus, M., Kirsch, K. & Westfall, J. (2012) *NACP aboveground biomass and carbon baseline data (NBCD 2000)*, USA 2000 data set. ORNL DAAC, Oak Ridge, TN. Available at: http://daac.ornl.gov (accessed 7 November 2012)

Köble, R. & Seufert, G. (2001) Novel maps for forest tree species in Europe. *Proceedings of the 8th European Symposium on the Physico-Chemical Behaviour of Air Pollutants: 'A Changing Atmosphere!'*, Torino, Italy, 17–20 September 2001.

Kurz, W.A., Dymond, C.C., Stinson, G., Rampley, G.J., Neilson, E.T., Carroll, A.L., Ebata, T. & Safranyik, L. (2008) Mountain pine beetle and forest carbon feedback to climate change. *Nature*, **452**, 987–990.

Lefsky, M.A., Cohen, W.B., Harding, D.J., Parker, G.G., Acker, S.A. & Gower, S.T. (2002) Lidar remote sensing of aboveground biomass in three biomes. *Global Ecology and Biogeography*, **11**, 393–399.

Liski, J., Korotkov, A.V., Prins, C.F.L., Karjalainen, T., Victor, D.G. & Kauppi, P.E. (2003) Increased carbon sink in temperate and boreal forests. *Climatic Change*, **61**, 89–99.

Lo, E. (2005) Gaussian error propagation applied to ecological data: post-ice-storm-downed woody biomass. *Ecological Monographs*, **75**, 451–466.

Mayaux, P., Eva, H., Gallego, J., Strahler, A.H., Herold, M., Agrawal, S., Naumov, S., De Miranda, E.E., Di Bella, C.M., Ordoyne, C., Kopin, Y. & Roy, P. (2006) Validation of the global land cover 2000 map. *IEEE Transactions on Geoscience and Remote Sensing*, **44**, 1728–1739.

Moorcroft, P.R., Hurtt, G.C. & Pacala, S.W. (2001) A method for scaling vegetation dynamics: the ecosystem demography model (ED). *Ecological Monographs*, **71**, 557–585.

Neumann, M., Saatchi, S.S., Ulander, L.M.H. & Fransson, J.E.S. (2012) Assessing performance of L- and P-Band polarimetric interferometric SAR data in estimating boreal forest aboveground biomass. *IEEE Transactions on Geoscience and Remote Sensing*, **50**, 714–726.

Olson, D.M., Dinerstein, E., Wikramanayake, E.D., Burgess, N.D., Powell, G.V.N., Underwood, E.C., D'Amico, J.A., Itoua, I., Strand, H.E., Morrison, J.C., Loucks, C.J., Allnutt, T.F., Ricketts, T.H., Kura, Y., Lamoreux, J.F., Wettengel, W.W., Hedao, P. & Kassem, K.R. (2001) Terrestrial ecoregions of the world: a new map of life on Earth. *Bioscience*, **51**, 933–938.

Pan, Y., Birdsey, R.A., Fang, J., Houghton, R., Kauppi, P.E., Kurz, W.A., Phillips, O.L., Shvidenko, A., Lewis, S.L., Canadell, J.G., Ciais, P., Jackson, R.B., Pacala, S.W., McGuire, A.D., Piao, S., Rautiainen, A., Sitch, S. & Hayes, D. (2011) A large and persistent carbon sink in the world's forests. *Science*, **333**, 988–993.

Patenaude, G., Hill, R.A., Milne, R., Gaveau, D.L.A., Briggs, B.B.J. & Dawson, T.P. (2004) Quantifying forest above ground carbon content using LiDAR remote sensing. *Remote Sensing of Environment*, **93**, 368–380.

Pinheiro, J. & Bates, D. (2000) *Mixed-effects models in S and S-PLUS*. Springer, New York.

Randerson, J.T., Hoffman, F.M., Thornton, P.E., Mahowald, N.M., Lindsay, K., Lee, Y.-H., Nevison, C.D., Doney, S.C., Bonan, G., Stöckli, R., Covey, C., Running, S.W. & Fung, I.Y. (2009) Systematic assessment of terrestrial biogeochemistry in coupled climate–carbon models. *Global Change Biology*, **15**, 2462–2484.

Ranson, K.J., Sun, G., Lang, R.H., Chauhan, N.S., Cacciola, R.J. & Kilic, O. (1997) Mapping of boreal forest biomass from spaceborne synthetic aperture radar. *Journal of Geophysical Research*, **102**, 29599–29610.

Saatchi, S.S., Houghton, R.A., Alvala, R.C.D., Soares, J.V. & Yu, Y. (2007) Distribution of aboveground live biomass in the Amazon Basin. *Global Change Biology*, **13**, 816–837.

Saatchi, S.S., Harris, N.L., Brown, S., Lefsky, M., Mitchard, E.T., Salas, W., Zutta, B.R., Buermann, W., Lewis, S.L., Hagen, S., Petrova, S., White, L., Silman, M. & Morel, A. (2011) Benchmark map of forest carbon stocks in tropical regions across three continents. *Proceedings of the National Academy of Sciences USA*, **108**, 9899–9904.

Santoro, M., Beer, C., Cartus, O., Schmullius, C., Shvidenko, A., McCallum, I., Wegmüller, U. & Wiesmann, A. (2011) Retrieval of growing stock volume in boreal forest using hyper-temporal series of Envisat ASAR ScanSAR backscatter measurements. *Remote Sensing of Environment*, **115**, 490–507.

Santoro, M., Cartus, O., Fransson, J.E.S., Shvidenko, A., McCallum, I., Hall, R.J., Beaudoin, A., Beer, C. & Schmullius, C. (2013) Estimates of forest growing stock volume for Sweden, Central Siberia and Québec using Envisat Advanced Synthetic Aperture Radar backscatter data. *Remote Sensing*, **5**, 4503–4532.

Saugier, B., Roy, J. & Mooney, H.A. (2001) Estimations of global terrestrial productivity: converging toward a single number?

Terrestrial global productivity (ed. by J. Roy, B. Saugier and H.A. Mooney), pp. 543–557. Academic Press, San Diego, CA.

Schepaschenko, D., Shvidenko, A. & Nilsson, S. (1998) Phytomass (live biomass) and carbon of Siberian forests. *Biomass and Bioenergy*, **14**, 21–31.

Schepaschenko, D., McCallum, I., Shvidenko, A., Fritz, S., Kraxner, F. & Obersteiner, M. (2011) A new hybrid land cover dataset for Russia: a methodology for integrating statistics, remote sensing and *in situ* information. *Journal of Land Use Science*, **6**, 245–259.

Shinozaki, K., Yoda, K., Hozumi, K. & Kira, T. (1964) A quantitative analysis of plant form – the pipe model theory. I. Basic analyses. *Japanese Journal of Ecology*, **14**, 97–105.

Shvidenko, A., Schepaschenko, D., Nilsson, S. & Bouloui, Y. (2007) Semi-empirical models for assessing biological productivity of northern Eurasian forests. *Ecological Modelling*, **204**, 163–179.

Shvidenko, A., Schepaschenko, D., McCallum, I. & Nilsson, S. (2010) Can the uncertainty of full carbon accounting of forest ecosystems be made acceptable to policymakers? *Climatic Change*, **103**, 137–157.

Somogyi, Z., Teobaldelli, M., Federici, S., Matteucci, G., Pagliari, V., Grassi, G. & Seufert, G. (2008) Allometric biomass and carbon factors database. *iForest – Biogeosciences and Forestry*, **1**, 107–113.

Taylor, J.R. (1997) *An introduction to error analysis. The study of uncertainties in physical measurements*. University Science Books, Sausalito, CA.

Teobaldelli, M., Somogyi, Z., Migliavacca, M. & Usoltsev, V.A. (2009) Generalized functions of biomass expansion factors for conifers and broadleaved by stand age, growing stock and site index. *Forest Ecology and Management*, **257**, 1004–1013.

Thomas, S.C. & Martin, A.R. (2012) Carbon content of tree tissues: a synthesis. *Forests*, **3**, 332–352.

UN-REDD (2011) *UN-REDD Programme. Support to National REDD+ Action*. Global Programme Framework 2011–2015. Adopted as of 9 August 2011. The United Nations Collaborative Programme on Reducing Emissions from Deforestation and Forest Degradation in Developing Countries.

USDA (2012) *Forest inventory and analysis national program*. United States Department of Agriculture. Available at: http://www.fia.fs.fed.us/ (accessed 7 November 2012).

Wagner, W., Luckman, A., Vietmeier, J., Tansey, K., Balzter, H., Schmullius, C., Davidson, M., Gaveau, D., Gluck, M., Le Toan, T., Quegan, S., Shvidenko, A., Wiesmann, A. & Yu, J.J. (2003) Large-scale mapping of boreal forest in Siberia using ERS tandem coherence and JERS backscatter data. *Remote Sensing of Environment*, **85**, 125–144.

Wolf, A., Ciais, P., Bellassen, V., Delbart, N., Field, C.B. & Berry, J.A. (2011) Forest biomass allometry in global land surface models. *Global Biogeochemical Cycles*, **25**, GB3015. doi:10.1029/2010GB003917.

Wood, S.N. (2006) *Generalized additive models: an introduction with R*. Chapman & Hall/CRC Press, Boca Raton, FL.

Wutzler, T., Wirth, C. & Schumacher, J. (2008) Generic biomass functions for common beech (*Fagus sylvatica*) in central Europe: predictions and components of uncertainty. *Canadian Journal of Forest Research*, **38**, 1661–1675.

Zanne, A.E., Lopez-Gonzalez, G., Coomes, D.A., Ilic, J., Jansen, S., Lewis, S.L., Miller, R.B., Swenson, N.G., Wiemann, M.C. & Chave, J. (2009) *Data from: towards a worldwide wood economics spectrum*. Dryad Digital Repository. Available at: http://datadryad.org/handle/10255/dryad.234 (accessed 2 November 2011).

Zianis, D., Muukkonen, P., Mäkipää, R. & Mencuccini, M. (2005) Biomass and stem volume equations for tree species in Europe. *Silva Fennica Monographs*, **4**, 63.

Zuur, A.F., Ieno, E.N., Walker, N.J., Saveliev, A.A. & Smith, G.M. (2009) *Mixed effects models and extensions in ecology with R*. Springer, New York.

SUPPORTING INFORMATION

Additional supporting information may be found in the online version of this article at the publisher's web-site.

Appendix S1 GLC2000 classes and their aggregation to leaf types.

Appendix S2 Spatial distribution of biomass compartment carbon density in Northern Hemisphere boreal and temperate forests and its corresponding relative uncertainty.

Appendix S3 Intercomparison of this study's (MPI) and IIASA forest enterprise carbon density data for different bioclimatic zones in Russia.

Appendix S4 Modelling of branch, root and foliage biomass out of stem biomass and other predictors using generalized additive models.

BIOSKETCH

Martin Thurner is a PhD student at Max Planck Institute for Biogeochemistry in Jena, Germany. His main research interest is to improve climate carbon cycle models by the integration of remote sensing data.

Editor: Josep Penuelas